Programmable bioelectronics in a stimuli-encoded 3D graphene interface†

Onur Parlak,‡[a] Selim Beyazit,[b] Bernadette Tse-Sum-Bui,[b] Karsten Haupt,[b] Anthony P. F. Turner[a] and Ashutosh Tiwari*[a,c,d]

The ability to program and mimic the dynamic microenvironment of living organisms is a crucial step towards the engineering of advanced bioelectronics. Here, we report for the first time a design for programmable bioelectronics, with 'built-in' switchable and tunable bio-catalytic performance that responds simultaneously to appropriate stimuli. The designed bio-electrodes comprise light and temperature responsive compartments, which allow the building of Boolean logic gates (*i.e.* "OR" and "AND") based on enzymatic communications to deliver logic operations.

In nature, living reactions are naturally programmed, and attempts to construct artificial biological systems have generally resulted in an inferior performance.[1-3] This biotechnological problem could be solved by the use of a programmable approach to segregate reaction conditions at a molecular level.[4] It is worth noting that a stimuli-encoded material as a trimming element could provide a way to regulate from the 'on-state' to an 'off-state' and/or to program the rate of biological reactions *via* slow-to-medium-to-high and *vice versa*.[5-7] There has been growing interest in switchable bio-catalysis in response to real-life chemical and physical stimuli as a new platform to understand control and regulation mechanisms underlying physiological processes.[8] Biochemical interactions and electron transfer phenomena that mimic biochemical reactions in living systems can be understood by controlling their environment and operations using external physical stimuli.[4,9,10] The modelling of physical interactions of bio-molecules in a confined volume has, for example, had significant impact on the efficiency of bio-catalysis and functional control using external stimuli such as light, temperature or magnetic fields.[8,9,11,12] Bio-molecular interactions involving non-covalent bonding, intermolecular forces and van der Waals interactions play an important role in bio-catalysis.[13] Hence, the control and regulation of these interactions dominate their functions. Likewise, electrochemical enzymatic devices offer a number of positive features including flexibility, choice of catalyst, variety of electrode systems and operation.[14-16] However, state-of-the-art enzymatic bio-devices have major limitations related to the lack of control and regulation mechanisms, electron transfer and mass transport efficiency, and enzyme immobilisation. In order to maximise performance and overcome technical hurdles, there is a need for the smart engineering of electrode materials.[4]

Here, we introduce two different model systems which allow one to program electrochemical output signals using both light irradiation and temperature change. Depending on the electrode design, Boolean logic gates (*i.e.*, "OR" and "AND") are built to generate programmable bio-electrodes to control and regulate bio-molecular interactions in accordance with logic operations.[6,7] The model systems consist of compartmentalised electrode surfaces containing acrylamide co-polymerised with light-responsive spiropyran methacrylate molecular units poly(Aam-*co*-SPMA) (PAA-*co*-SPMA), which are assembled together with pyrroloquinoline quinone (PQQ)-dependent glucose dehydrogenase (GDH) immobilised on graphene in one compartment, and temperature-responsive amine-terminated poly(*N*-isopropylacrylamide) assembled with cholesterol oxidase (ChOx) immobilised graphene in another compartment. In this prototype, the electrochemical output signal is controlled in the presence of two substrates, glucose and cholesterol. The mechanism in the light-responsive compartment is based on the isomerisation of the spiropyran (SP) unit in the polymeric chain. Here, SP units are converted to the charge-separated open-ring isomeric form of merocyanine (MC) upon exposure to UV-light. This isomerisation induces structural permeability and polarity differences between the two forms of the polymers, which result in a substantial

[a]Biosensors and Bioelectronics Centre, IFM, Linköping University, 581 83 Linköping, Sweden. E-mail: ashutosh.tiwari@liu.se
[b]Sorbonne Universités, Université de Technologie de Compiègne, CNRS Laboratory for Enzyme and Cell Engineering, CS60319, 60203 Compiègne Cedex, France
[c]Tekidag AB, UCS, Teknikringen 4A, Mjärdevi Science Park, Linköping 583 30, Sweden
[d]Vinoba Bhave Research Institute, Sirsa Road, Saidabad, Allahabad 221508, India
†Electronic supplementary information (ESI) available. See DOI: 10.1039/c6nr02355j
‡Present address: Department of Materials Science and Engineering, Stanford University, 476 Lomita Mall, Stanford, 94305 California, USA

change in electrical properties. Under UV-light (*i.e.*, ≤ 385 nm), SP undergoes a ring-opening conformation, which induces volume and polarity changes.[17–19] These changes result in an increased permeability of the polymer membrane towards the bio-substrate (*i.e.*, a volume effect) and an increase in the ionic conductivity of the interface due to the charge separation, which mainly results from the large electric dipole moment difference between the MC and SP states (*i.e.*, a polarity effect).[12,20] In contrast, at relatively long wavelengths of light (*i.e.*, ≥420 nm), SP forms a spiropyran-functionalised polymer densely packed at the electrode edges, which results in a lower permeability and diffusion of the bio-substrate and thus suppresses the electrochemical signals. The mechanism in the temperature-responsive compartment on the other hand, is based on the reversible formation of hydrogen bonding between graphene and the polymer. Here, the interaction between graphene and the polymer shows distinctive behaviours at two different temperatures. At a relatively low temperature (*i.e.*, at 20 °C), the formation of hydrogen bonding creates a coalescence between the surfaces, thereby causing significant shrinkage in the graphene–polymer matrix. Thus, access of an associated enzyme to its substrate is largely restricted, resulting in a decrease in the diffusion of reactants and the consequent lowering of the system's activity. However, at a comparatively high temperature (*i.e.*, at 40 °C) the hydrogen bonding interaction is subverted. As a result, the bio-substrate, cholesterol, can easily access the enzyme to facilitate bioelectrocatalysis. More importantly, in the proposed model both responsive compartments can be controlled simultaneously.

In order to obtain 3D graphene, we first modified the surface of graphene with a negatively charged surfactant, sodium dodecyl benzene sulphonate (SDBS) to prevent the aggregation of individual sheets and direct the assembly of enzymes and polymers for further immobilisation (Fig. S1, ESI†). The results showed that graphene nanosheets, after surface modification, produced wrinkled structures and a low degree of aggregation in the graphene nanosheets. After enzyme immobilisation, a high resolution TEM image was taken to show successful assembling. Although the high resolution TEM image of a ChOx immobilised graphene hybrid structure (Fig. S2, ESI†) showed good homogeneity and dispersion, it was still difficult to resolve enzyme structures in these images. Finally, after assembling graphene–enzyme, the 3D assembly was completed by incorporating the light and temperature-responsive polymers. Fig. 1 represents SEM images of hybrid structures prepared as a hierarchical self-assembly using a GDH-modified graphene hybrid structure conjugated with light-responsive PAA-*co*-SPMA (a) and the ChOx-immobilised temperature-responsive PNIPAAM graphene (b). The samples were prepared by taking a drop of each solution and casting it on a holder, followed by drying overnight. These images show that there is a low degree of aggregation, which is probably due to the centrifugation during the preparation process. These figures also show us homogeneous dispersion and that 3D structures have been achieved using graphene–enzyme and polymer units.

The initial reaction system includes both 5 mM glucose, and 5 mM cholesterol and 0.1 M KCl as a supporting electrolyte dissolved in 10 mM PBS, pH 7.4. In contrast to common approaches, the bio-electrodes are programmed using light irradiation and temperature change as input signals, which are able to 'activate' and/or 'deactivate' individual reactions of the one-to-one compartment. Each design offers a bioelectronics set-up composed of "AND" and "OR" gates. The physical
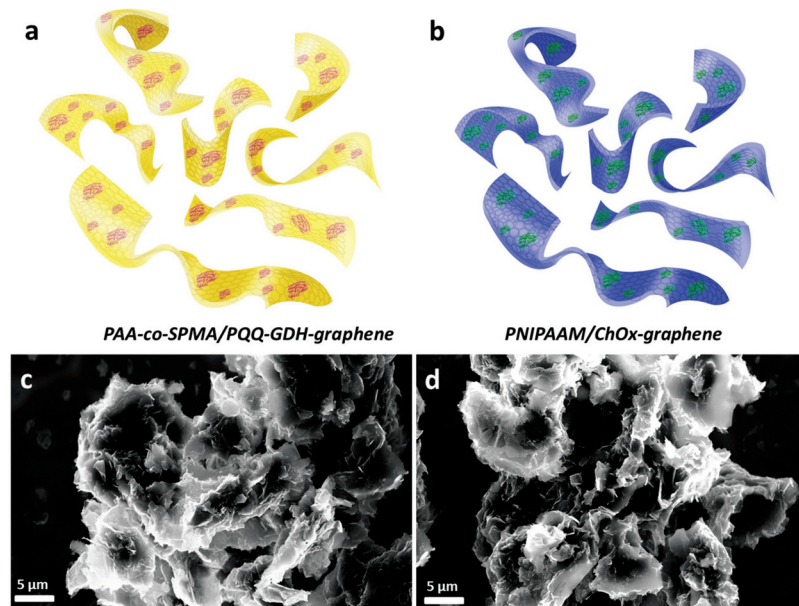

Fig. 1 Schematic illustration of (a) PQQ-GDH immobilised light-responsive PAA-*co*-SPMA graphene, (b) ChOx loaded temperature-responsive PNIPAAM graphene, and their SEM images (c) and (d), respectively.

input signals for the system are considered as "1" when they are applied (*i.e.*, UV-light and 40 °C) and "0" if they are not applied to the system (*i.e.*, visible-light and 20 °C). The output signal of the concatenated gate is measured as the electrochemical signal corresponding to each enzymatic reaction.

Fig. 2a illustrates our "AND" gate concept. A patterned compartment of graphene mixed with the temperature-responsive polymer–cholesterol oxidase hybrid was first immobilised on a gold electrode. Then, a light-responsive polymer–glucose dehydrogenase mixture is covalently bonded as a second layer to
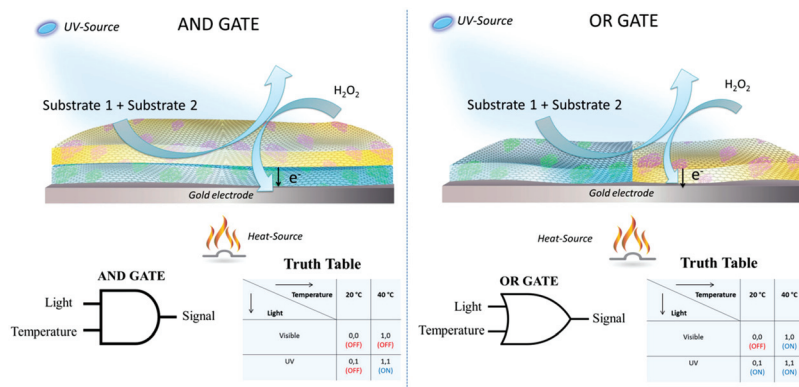

Fig. 2   Logic gate designs for programmable bio-electrodes. "AND" gate and related 'Truth Table' (a), and "OR" gate and related 'Truth Table' (b).
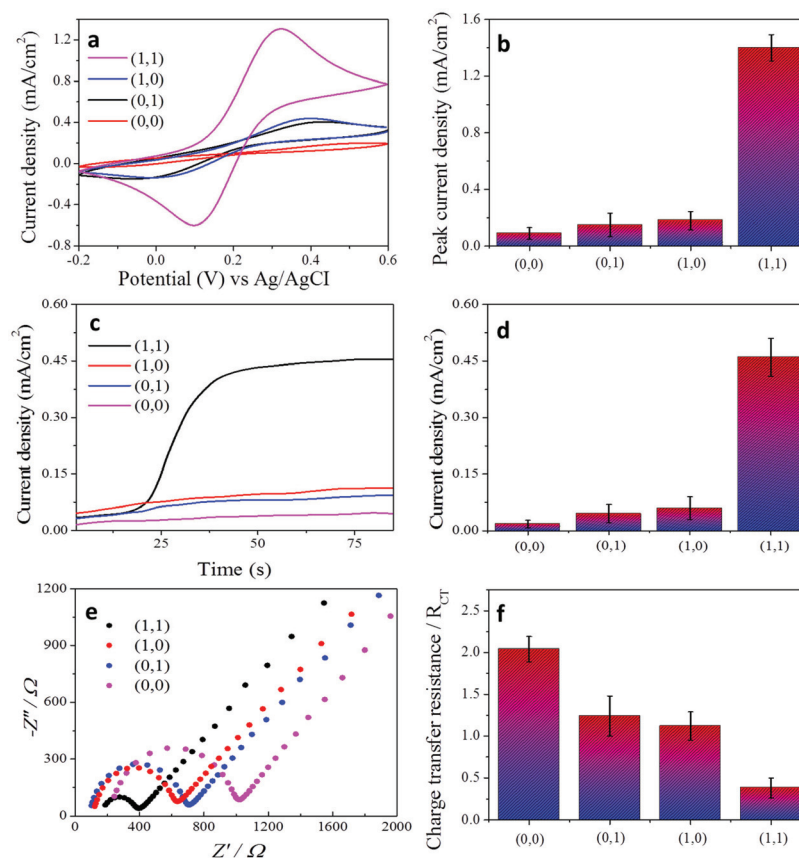

Fig. 3   Electrochemical characterisation of the "AND" gate design. Cyclic voltammetry responses (a) and the peak potential chart (b), chrono-amperometric responses (c) and steady-state current density charts (d), impedimetric responses (e) and charge-transfer resistance (R_{CT}) charts (f) for all conditions in the "AND" gate design. All cyclic voltammetry and impedance measurements were carried out in 5 mM $[Fe(CN)_6)]^{3-/4-}$ and 0.1 M PBS *vs*. the Ag/AgCl reference electrode. The scan rate for voltammetric measurements is 50 mV s^{-1}. The chronoamperometric results were obtained under the same conditions with cyclic voltammetry and impedance measurements and additionally in the presence of 5 mM glucose and 5 mM cholesterol under the stated conditions at 0.4 V applied voltage.

the top of the first compartment. Here, we have studied the logic responses of the system on the external signals encoded by physical stimuli. The experimental electrochemical signals based on amperometric and voltammetric results obtained upon four different combinations of input signals "0" and "1" are shown in the 'Truth Table' in Fig. 2a. The responses obtained from the system correspond to the 'Truth Table' expected for the sequence of the concatenated "AND" gates. For the "AND" gate, only one correct order (1,1) of the input signals resulted in the "TRUE" or "ON" state output signal "1", while the others produced "FALSE" or "OFF" state output signal "0".

In order to prove the concept, we performed a set of experiments when the order of the stimuli-encoded input signals was varied in different combinations. All the electrochemical experiments were carried out in the presence of 5 mM $[Fe(CN)_6]^{3-/4-}$ aqueous solution for voltammetric measurements

(Fig. 3a) and in the presence of 5 mM cholesterol and 5 mM glucose in PBS solution, pH 7.4 for amperometric measurements (Fig. 3c). In the operation designated as (0,0), electrochemical measurements were carried out at 20 °C and under day-light, which results in no electrochemical signal. When only temperature (1,0) or only UV-light (0,1) stimuli are applied to the system, the corresponding electrochemical signal cannot be generated due to the design of the bioelectrode. In the operation (1,0), even if the system is heated to 40 °C and the temperature compartment is ready to interact, the conformation of the light-responsive part does not allow biomolecules or electroactive redox species to diffuse through the temperature-responsive compartment, which brings significant suppression of the electrochemical signal. However, when we order a "TRUE" operation (1,1), electrochemical signals are significantly increased in both the amperometric and voltammetric measurements. Under UV-irradiation and
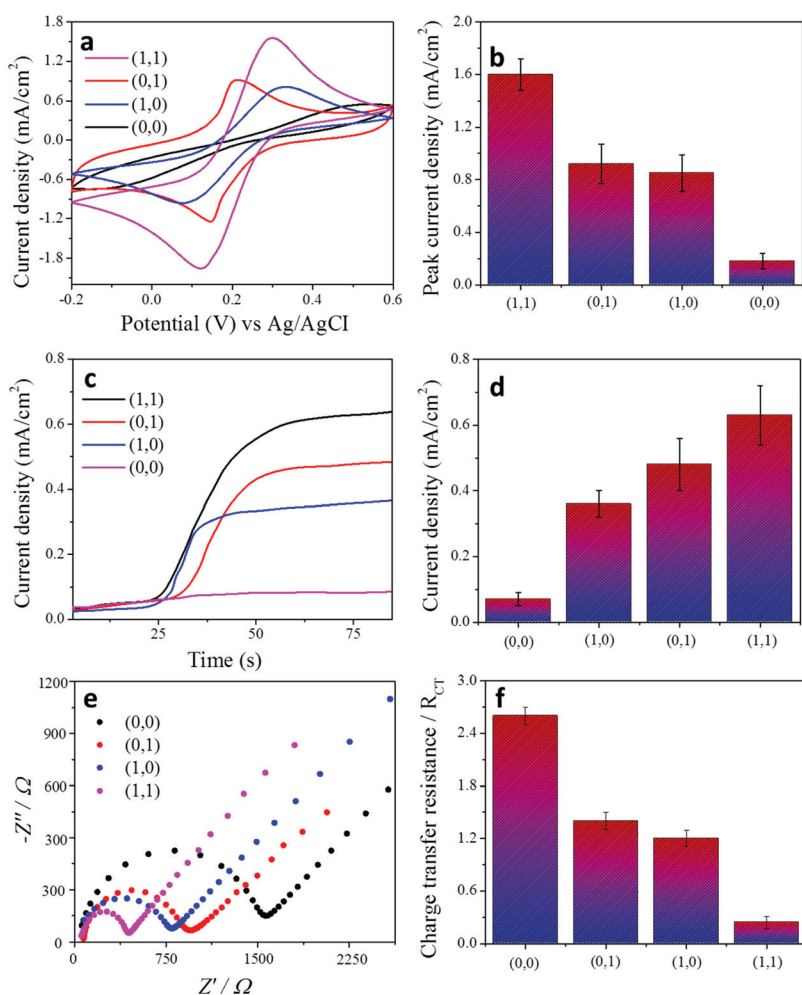

Fig. 4 Electrochemical characterisation of the "OR" gate design. Cyclic voltammetry responses (a) and peak potential chart (b), chronoamperometric responses (c) and steady-state current density charts (d), impedimetric responses (e) and charge-transfer resistance (R_{CT}) charts (f) for all conditions in the "AND" gate design. All cyclic voltammetry and impedance measurements were carried out in 5 mM $[Fe(CN_6)]^{3-/4-}$ and 0.1 M PBS vs. the Ag/AgCl reference electrode. The scan rate for voltammetric measurements is 50 mV s^{-1}. The chronoamperometric results were obtained under the same conditions with cyclic voltammetry and impedance measurements and additionally in the presence of 5 mM glucose and 5 mM cholesterol under the stated conditions at 0.4 V applied voltage.

40 °C, the system design allows cholesterol molecules to pass through the temperature-responsive compartment and allows glucose to react with glucose dehydrogenase in the light-responsive matrix. Eventually, cholesterol can diffuse through the bottom layer and produce an electrochemical signal.

In addition to amperometric and voltammetric measurements, the charge-transfer properties of each condition for the "AND" and "OR" gates were characterised by electrochemical impedance spectroscopy (Fig. 3e and f and Fig. 4e and f). A Randles circuit was chosen to fit the impedance output. The results are shown as Nyquist plots of spectra which contain semi-circular and linear portions. The charge-transfer resistance (R_{CT}) of each condition was calculated based on the diameter of the semi-circular part of the plot (ESI Fig. 3†).

Fig. 2b illustrates our "OR" gate concept. In order to construct the "OR" gate, the electrode design is changed. The same light and temperature responsive compartments which were used in the "AND" gate design were tested here. First, a patterned compartment of graphene, mixed with the temperature-responsive polymer–cholesterol oxidase 3D hybrid is covalently attached to one side of a gold electrode and the light-responsive polymer–glucose dehydrogenase mixture is covalently bonded to the other side of the electrode, as described in Fig. 2b. The logic responses of the system to the external signals encoded by physical stimuli were studied. The experimental electrochemical signals based on amperometric and voltammetric results obtained upon four different combinations of input signals "0" and "1" are shown in Fig. 4a–f. The responses obtained from the system correspond to the 'Truth Table' expected for the sequence of the concatenated "OR" gates. For the "OR" gate, there are three correct orders (1,0), (0,1) and (1,1) of the input signals resulting in the "TRUE" or "ON" state output signal "1", while the other one produced a "FALSE" or "OFF" state output signal "0". The only "FALSE" operation designated as (0,0) resulted in no electrochemical signal. When only a temperature (1,0) or only a light (0,1) stimulus is applied to the system the corresponding electrochemical signal can be generated accordingly. In the operation "1,0" or "0,1", the system is either heated at 40 °C or irradiated with UV-light; the temperature compartment or light-responsive compartment is ready to interact even if the complementary part is closed to biomolecules and the electroactive redox species can easily diffuse through the corresponding compartment, which results in the generation of an electrochemical signal. When we order a "TRUE" operation (1,1), electrochemical signals are significantly increased in both the amperometric and voltammetric measurements. Under UV-irradiation and 40 °C, the system design allows both cholesterol and glucose molecules to pass through to each compartment and permits them to react with cholesterol oxidase and glucose dehydrogenase in the corresponding compartment. Eventually, both temperature and light-responsive compartments allow the diffusion of biomolecules and enable the generation of electrochemical signals. The repeatability of each system was studied and results are demonstrated in the ESI figure.†

Experimental section

3D assembly of functional graphene

Graphene nanosheets were produced using the Hummers method (Graphene Supermarket, USA) and graphene-based bioconjugates containing graphene–pyrroloquinone quinone-dependent glucose dehydrogenase (PQQ-dependent GDH, from *Acinetobacter calcoaceticus*), and graphene–cholesterol oxidase (ChOx, from *Streptomyces* sp.) were prepared separately according to previously published reports, with minor modifications.[21–23] Then, GDH-immobilised graphene and ChOx-immobilised assemblies were incorporated into amine-terminated PNIPAAM and spiropyran methacrylate polyacrylamide functionalised co-polymerised polyacrylamide (poly(Aam-co-SPMA)), respectively. In a typical mixture, 1 mg of ChOx–graphene and GDH–graphene were added to 1 mL of 1 mg PNIPAAM and poly(Aam-co-SPMA) aqueous solutions to form a homogeneous suspension with ultrasonication, respectively.

Fabrication of the switchable bio-electrode

Prior to coating, gold electrodes were polished using 1.0, 0.3, and 0.05 microns Buehler alumina slurry on a Buehler polishing microcloth (Buehler Ltd, USA), respectively. The electrodes were then cleaned in a mixture of aqueous ammonia, hydrogen peroxide and water solution (1 : 1 : 5 v/v) at 80 °C for 10 min and rinsed with excess deionised water. The electrodes were electrochemically cleaned in 0.05 M H_2SO_4 solution by cycling between 0.0 V to 1.5 V and allowed to dry at room temperature. For the "AND" gate design, the first temperature responsive matrix containing ChOx–graphene and PNIPAAM was drop-cast on the electrode surface, then as a second layer, the light-responsive unit was electrostatically assembled on the first layer. In the "OR" gate design, the electrode surface was equally divided and each area was immobilised with the corresponding responsive-matrices.

Conclusions

In summary, we introduced for the first time the concept of a programmable bioelectronics controlled by external physical stimuli as a viable route to achieve the necessary enhanced performance using "switchable" and "smart" bioelectrodes for both fundamental and applied studies of high-performance bioelectronics. As a first demonstration, we utilised 3D graphene based smart bioelectrodes, which possess the finest triggered textural ability to control biological reactions. The programming of prototype bioelectronic devices was demonstrated *via* 'built-in' switchable and tunable biocatalysis that respond instantaneously to appropriate stimuli through "AND" and "OR" logic gates. It was tested in parallel with a target substrate, glucose and cholesterol in two sequential compartments on one electrode. These smart bioelectrocatalytic methods are promising candidates to provide key building blocks for future hands-on mimetic biosystems, as well as ideal protocols for fundamental research.

Acknowledgements

Notes and references

1 A. P. F. Turner, *Chem. Soc. Rev.*, 2013, **42**, 3184–3196.
2 A. P. F. Turner, *Science*, 2000, **290**, 1315–1317.
3 A. Noy, *Adv. Mater.*, 2011, **23**, 807–820.
4 O. Parlak and A. P. F. Turner, *Biosens. Bioelectron.*, 2016, **76**, 251–265.
5 O. Parlak, A. P. F. Turner and A. Tiwari, *J. Mater. Chem. B*, 2015, **3**, 7434–7439.
6 O. Parlak, S. Beyazit, B. Tse Sum Bui, K. Haupt, A. Tiwari and A. P. F. Turner, *Adv. Mater. Interfaces*, 2016, **3**, 1500353.
7 O. Parlak, A. P. F. Turner and A. Tiwari, *Adv. Mater.*, 2014, **26**, 482–486.
8 E. Katz and V. Privman, *Chem. Soc. Rev.*, 2010, **39**, 1835–1857.
9 M. Privman, T. K. Tam, M. Pita and E. Katz, *J. Am. Chem. Soc.*, 2009, **131**, 1314–1321.
10 I. Tokarev, V. Gopishetty, J. Zhou, M. Pita, M. Motornov, E. Katz and S. Minko, *ACS Appl. Mater. Interfaces*, 2009, **1**, 532–536.
11 E. Katz, V. Bocharova and M. Privman, *J. Mater. Chem.*, 2012, **22**, 8171–8178.
12 P. M. Mendes, *Chem. Soc. Rev.*, 2008, **37**, 2512–2529.
13 O. Parlak, A. Tiwari, A. P. F. Turner and A. Tiwari, *Biosens. Bioelectron.*, 2013, **49**, 53–62.
14 M. J. Cooney, V. Svoboda, C. Lau, G. Martin and S. D. Minteer, *Energy Environ. Sci.*, 2008, **1**, 320–337.
15 S. C. Barton, J. Gallaway and P. Atanassov, *Chem. Rev.*, 2004, **104**, 4867–4886.
16 Y. Wang, Z. H. Li, J. Wang, J. H. Li and Y. H. Lin, *Trends Biotechnol.*, 2011, **29**, 205–212.
17 R. Klajn, *Chem. Soc. Rev.*, 2014, **43**, 148–184.
18 J. J. Davis, D. A. Morgan, C. L. Wrathmell, D. N. Axford, J. Zhao and N. Wang, *J. Mater. Chem.*, 2005, **15**, 2160–2174.
19 W. R. Browne and B. L. Feringa, in *Annual Review of Physical Chemistry*, 2009, vol 60, pp. 407–428.
20 P. M. Mendes, *Chem. Soc. Rev.*, 2013, **42**, 9207–9218.
21 G. Goebel, I. W. Schubart, V. Scherbahn and F. Lisdat, *Electrochem. Commun.*, 2011, **13**, 1240–1243.
22 O. Parlak, P. Seshadri, I. Lundstrom, A. P. F. Turner and A. Tiwari, *Adv. Mater. Interfaces*, 2014, 1.
23 J. Razumiene, A. Vilkanauskyte, V. Gureviciene, J. Barkauskas, R. Meskys and V. Laurinavicius, *Electrochim. Acta*, 2006, **51**, 5150–5156.